AGU100 ADVANCING EARTH AND SPACE SCIENCE

Water Resources Research

RESEARCH ARTICLE
10.1002/2017WR021662

Key Points:
- Examine the conditional role of individual and joint factors in compound events via the conditional framework of vine copula
- Address the interrelationship not only between extreme variables and physical conditions but also between the conditions themselves
- The individual variable of precipitation and runoff may not itself be extreme, but large exceedances can lead to flooding when combined

Supporting Information:
- Supporting Information S1

Correspondence to:
L. Cheng,
linyin.cheng@noaa.gov

Citation:
Liu, Z., Cheng, L., Hao, Z., Li, J., Thorstensen, A., & Gao, H. (2018). A framework for exploring joint effects of conditional factors on compound floods. *Water Resources Research*, *54*. https://doi.org/10.1002/2017WR021662

Received 4 AUG 2017
Accepted 7 MAR 2018
Accepted article online 30 MAR 2018

© 2018. American Geophysical Union. All Rights Reserved.

A Framework for Exploring Joint Effects of Conditional Factors on Compound Floods

Zhiyong Liu[1,2,3], Linyin Cheng[4], Zengchao Hao[5], Jingjing Li[6], Andrea Thorstensen[7], and Hongkai Gao[8]

[1]Department/Center of Water Resources and Environment, Sun Yat-sen University, Guangzhou, China, [2]Guangdong Engineering Technology Research Center of Water Security Regulation and Control for Southern China, Sun Yat-sen University, Guangzhou, China, [3]Cooperative Institute for Research in the Atmosphere, Colorado State University, Fort Collins, CO, USA, [4]Cooperative Institute for Research in Environmental Sciences, University of Colorado, Boulder, CO, USA, [5]Green Development Institute, College of Water Sciences, Beijing Normal University, Beijing, China, [6]Department of Geosciences and Environment, California State University Los Angeles, Los Angeles, CA, USA, [7]National Research Council, National Oceanic and Atmospheric Administration/Earth System Research Laboratory, Boulder, CO, USA, [8]Julie Ann Wrigley Global Institute of Sustainability, Arizona State University, Tempe, AZ, USA

Abstract This study highlights the features of vine copula for examining compound events involving underlying conditions that amply the compounding effects. To illustrate, we study compound floods in Texas (TX), USA. These compound floods consist of combinations of precipitation and surface runoff with the El Niño-Southern Oscillation (ENSO) and rising temperatures as underlying conditions. Although the individual variable of precipitation and runoff may not itself be extreme, large exceedances can lead to flooding situations when combined. The presence of underlying conditions (e.g., El Niño and/or rising temperatures) can exacerbate the associated flood impacts. We use observational data during May–August for each climate division of TX. A three-dimensional vine copula is used first to quantify the ENSO effect on precipitation and runoff through conditioning sets of vine copula. We further examine the interplay of a warming signal and El Niño to reveal their mutual effects on compound floods by placing these two factors as interrelated conditions in a four-dimensional vine copula. Our results show that El Niño is much stronger than the other ENSO states in conditioning a high likelihood of TX compound floods by amplifying mean and extreme states of rainfall and runoff. Conditioned by both El Niño and global temperatures, a slight reduction occurs in TX compound floods under the warmer condition. This is consistent with the trend of precipitation and runoff composites under given conditions, while no appreciable changes are found to suggest a different joint effect of El Niño and rising temperatures on TX compound floods.

1. Introduction

Extreme impacts of weather and climate events, highlighted by Leonard et al. (2014), can result from either a single variable being in an extreme state or an accumulation of variables not all of which are extreme. The latter case is known as compound events. According to the Intergovernmental Panel on Climate Change (IPCC) report (Seneviratne et al., 2012), compound events are defined as: "(1) two or more extreme events occurring simultaneously or successively; (2) combinations of extreme events with underlying conditions that amplify the impact of the events; (3) combinations of events that are not themselves extremes but lead to an extreme event or impact when combined." Although awareness has increased about multivariate extreme events, compound events involving the (2) and (3) characteristics above receive little attention due to the limitations of current approaches and concepts.

Understanding the role of underlying conditions is important given the amplifying effects that they can bring to compound events (Dole et al., 2011; Lott et al., 2013; Pall et al., 2011; Stott et al., 2004; Trenberth et al., 2015). For instance, Prosdocimi et al. (2015) find substantially increased urbanization conditions to enhance the likelihood of urban floods by driving long-term changes of flows at catchments in northwestern England. Likewise, studies reveal that soil moisture content can be a strong conditioning factor for development of mega-heat waves in many regions of the world through land-atmosphere feedback (Mueller & Seneviratne, 2012). These compound events are conditioned by a single factor (i.e., urbanization level

or soil moisture state). It is also likely that multiple interrelated factors exert conditional effects and lead to more severe compound events (Field et al., 2012; Fischer et al., 2007; Leonard et al., 2014; Moftakhari et al., 2017; Stocker et al., 2013). In the case of sea level rise, the interplay of tide and surge conditions has significantly accelerated the sea level rise over the 20th century (Church & White, 2006). A transformed El Niño teleconnection related to the interaction between El Niño dynamics and anthropogenic forcing was found to be responsible for the floods over the southern Great Plains in May 2015 (Wang et al., 2015). Multiple interrelated conditions add another dimension to the analysis of compound events—the interdependency between underlying conditions affects whether their mutual interaction results in a damping or enhancement of the compounding effects.

To identify the contribution of underlying conditions, one needs to establish conditional relationship, which measures dependence of the occurrence or impact of one event on the occurrence of another event (Leonard et al., 2014; Seneviratne et al., 2012). A common approach for deriving conditional dependence applies composite analysis. For instance, precipitation composites are made for examining sensitivity of precipitation to different phases of El Niño-Southern Oscillation (ENSO) (e.g., Hendon, 2003; Wu et al., 2003). In this approach, the linkage between variables and underlying conditions is expressed in an empirical manner, therefore not sufficient to yield predictive information. Another approach is to perform linear regression (e.g., Lloyd, 2005). Assuming a linear relationship between variables and conditioning factors may be useful for describing changes related to variables' mean states (Mueller & Seneviratne, 2012), but for interpreting extreme tail behavior, the simplified assumption of linearity is questionable. More advanced methods, such as hidden Markov modeling, build such relationships through a doubly embedded stochastic process, producing a sequence of observations under the assumption of conditional independence of the hidden stochastic process (MacDonald & Zucchini, 1997). A Bayesian concept (Madadgar et al., 2016; Madadgar & Moradkhani, 2013; Sadegh et al., 2017) and the framework developed by Heffernan and Tawn (2004) for modeling multivariate extreme values with conditions can also be applied to estimate conditional distribution of random variables. A limitation of the latter two methods is that without assuming a specific dependence structure, there is no simple closed-form conditional distribution.

Copula has emerged as an effective approach for addressing interdependence between multiple variables (Salvadori et al., 2007). There are many applications of copula (e.g., Chebana & Ouarda, 2011; Cheng et al., 2016; De Michele & Salvadori, 2003; Favre et al., 2004; Hao & Singh, 2013, 2016; Khedun et al., 2014; Madadgar & Moradkhani, 2011, 2013; Salvadori et al., 2013, 2011; Sarhadi et al., 2016; Serinaldi et al., 2009; Vandenberghe et al., 2011). Most of these studies are in the context of unconditional assessment. In other words, no conditional relationships are invoked. Vine copula, also known as pair-copula construction, provides a solution for constructing multidimensional copula without requiring a conditional independence assumption (Aas et al., 2009). A few recent studies have demonstrated the applicability of vine copula to hydrology (e.g., Bevacqua et al., 2017; Xiong et al., 2015). These studies show the flexibility of vine copula in reproducing a wide range of dependence between multivariate variables, including heterogeneous dependence that could exist among different pairs (also see Liu et al., 2015, 2016; Vernieuwe et al., 2015; Xiong et al., 2014). Our purpose in this study is to highlight its usefulness for evaluating the importance of conditional relationships not only between variables and underlying conditions but also between the conditions themselves. The latter point is critical for examining compounding impacts caused by the mutual interaction of physical conditions, which can otherwise remain undetectable if these conditions are evaluated separately.

We employ the framework of vine copula for assessing compound floods over Texas (TX), USA. Our compound floods consist of combinations of precipitation and surface runoff with the El Niño-Southern Oscillation and rising temperature conditions, a scenario related to type (2) compound events in the IPCC report. It is well-known that ENSO affects extreme weather worldwide (e.g., Horel & Wallace, 1981; Hoskins & Karoly, 1981; Webster 1981) including changes in precipitation anomalies on daily to intraseasonal time scales in the southern and central USA. (e.g., Gershunov, 1998; Gershunov & Barnett, 1998; Hoell et al., 2015; Ropelewski & Halpert, 1986). In this study, we examine the conditional effect of ENSO for TX precipitation and surface runoff through the conditioning set of a three-dimensional vine copula. Surface temperature is another factor that is closely associated with variations in precipitation because of their thermodynamic relations (Adler et al., 2008; Allan & Soden, 2008). Moreover, emerging research indicates that an increase in global temperatures may intensify El Niño dynamics (e.g., Cai et al., 2015; Collins et al., 2010; Latif & Keenlyside, 2009; Meehl & Teng, 2007; Timmermann et al., 1999). Herein we examine the interplay of a warming

signal and El Niño to reveal their mutual effects on TX compound floods by placing these two factors as interrelated conditions using a four-dimensional vine copula.

We focus on May–August averaged precipitation and surface runoff for TX. Although the individual variable of precipitation and runoff may not itself be extreme, large exceedances can lead to flooding when combined. From this perspective, our study is also relevant for understanding type (3) compound events in the IPCC report. We apply this framework to 10 climate divisions of TX to identify changes in the spatial pattern of precipitation and surface runoff under corresponding climatic conditions. The description of our data and methods appears in section 2. We describe the results in section 3 and discuss implications in the last section.

2. Data and Methods

2.1. Data

Contiguous U.S. precipitation and surface runoff are obtained from National Oceanic and Atmospheric Administration (NOAA) monthly U.S. Climate Division data (NCDC, 2002). The monthly estimations of runoff were produced by a one-layer leaky bucket model driven with observed precipitation and temperature at

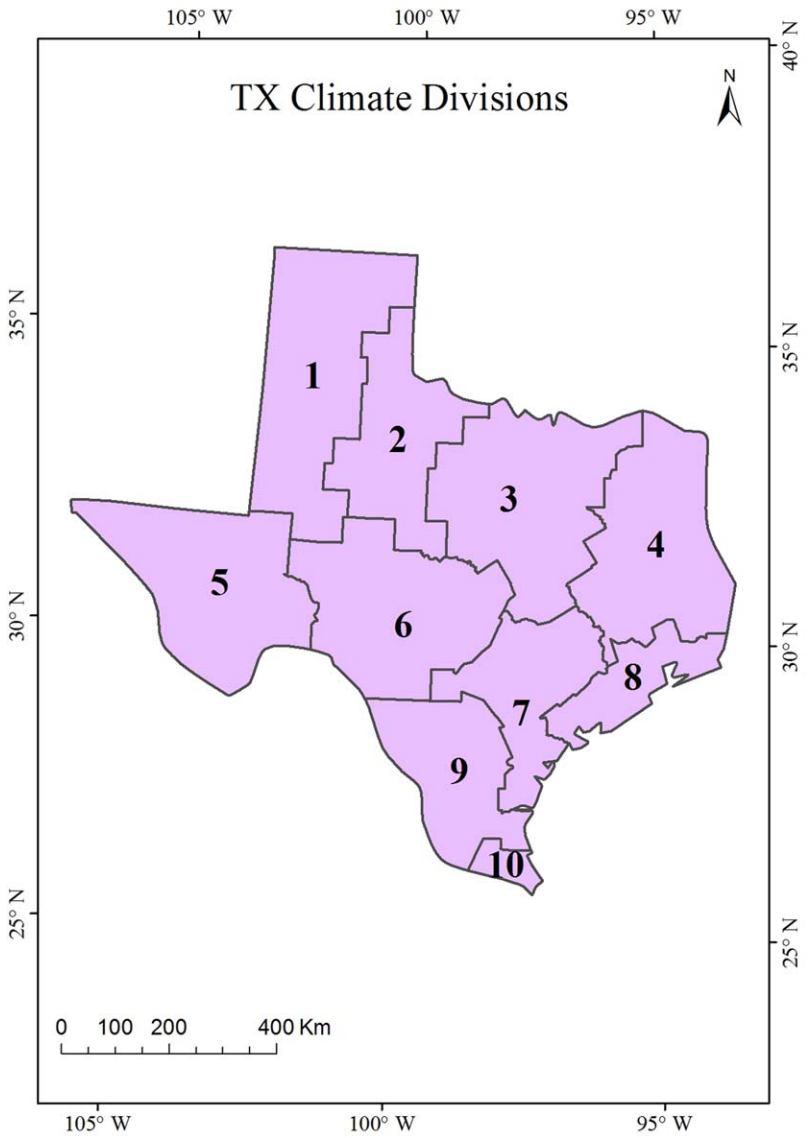


Figure 1. Ten climate divisions of Texas (TX) state, USA.

each climate division (Huang et al., 1996). We use data from 1932 to 2011, a period with complete annual monthly values for both precipitation and runoff. The availability of a relatively long record of these variables can facilitate a statistically robust estimate of changes in tail events. We focus on monthly rainfall and runoff averaged for the wet season, i.e., May–August, when TX receives approximately 60% of its annual precipitation and there is a high probability of compound flooding. Precipitation and runoff anomalies are first calculated relative to their respective May–August climatology (1932–2011) and then standardized with respect to one standard deviation of their univariate distribution during the wet season for each climate division of TX. Figure 1 shows the 10 climate divisions.

ENSO events during 1932–2011 are identified based on an averaged May–August exceedance of sea surface temperature (SST) anomalies in the Niño3.4 region (5°S–5°N, 170°W–120°W) relative to a 1932–2011 climatology (Climate Prediction Center, 2015; Kousky & Higgins, 2007). We define SST anomalies more than one standard deviation above (below) the long-term mean as El Niño (La Niña) and the rest as ENSO neutral cases in order to examine their respective effects on TX climate-division-based precipitation and surface runoff.

Global temperature is obtained from the HadCRUT4 data set at the Met Office Hadley Centre. The HadCRUT4 near surface temperature data set was produced by blending data from the Climatic Research Unit at the University of East Anglia (CRUTEM4) surface air temperature data set and the Hadley Centre SST (HadSST3) sea-surface temperature data set. A gridded data set of global historical surface temperature anomalies relative to a 1961–1990 reference period is available for each month since January 1850, on a 5° grid. Averaged May–August temperature anomalies from 1932 to 2011 are used for examining the combined impacts of El Niño and global temperature on compound floods.

2.2. Methods

2.2.1. Copula

Let $\boldsymbol{X} = (X_1, \ldots, X_d)^T$ be a d-dimensional random vector with joint distribution $F(x)$ and the marginal distributions $F_1(x_1), \ldots, F_d(x_d)$. According to Sklar's theorem (Sklar, 1959), there always exists a copula C which allows for joining the margins and modeling the joint dependence structure such that for all $(x_1, \ldots, x_d) \in (-\infty, \infty)^d$:

$$F(x_1, \ldots, x_d) = C(F_1(x_1), \ldots, F_d(x_d)) = C(u_1, \ldots, u_d) \tag{1}$$

where the copula C is a multivariate distribution function with uniform margins $(u_1, \ldots, u_d) \in [0, 1]^d$. The corresponding multivariate density can be expressed as (Yan, 2007):

$$f(x_1, \ldots, x_d) = \left[\prod_{i=1}^{d} f_i(x_i)\right] \times c(u_1, \ldots, u_d) \tag{2}$$

Table 1
Chi-Square Test for Different Theoretical Distributions Fitted to Runoff, Precipitation and SST Composites at Climate Division 5 (D5), With Respect to La Nina, ENSO Neutral and El Niño States

Distributions	Precipitation	SST	Runoff
		La Nina	
Normal	2.01	1.55	4.30
Gamma	2.08	1.50	4.00
Lognormal	2.12	**1.47**	**3.87**
Weibull	**1.98**	3.47	6.00
		ENSO Neutral	
Normal	12.15	4.32	9.46
Gamma	13.41	4.27	8.46
Lognormal	14.13	**4.26**	**8.08**
Weibull	**9.34**	6.94	23.06
		El Niño	
Normal	0.89	2.62	5.02
Gamma	0.83	2.50	4.51
Lognormal	**0.82**	**2.44**	**4.32**

Note. The best distribution for each variable is indicated in bold.

where $c(u_1, \ldots, u_d)$ and $f_i(x_i)$ represent the copula density and the marginal density, respectively. In this paper, we consider four univariate probability distributions as the potential margin of climate variables including May–August averaged rainfall and surface runoff at each climate division of TX, three phases of ENSO signal and the global averaged temperature during the same period. The best fit marginal distribution for each variable is identified according to the chi-square goodness of fit test (see Tables 1 and 2 as an example).

2.2.2. Vine Copula

Although parameter restrictions and computationally intensive formulations limit multivariate modeling at higher dimensions, e.g., $d \geq 3$ (Kurowicka, 2011; Ren et al., 2014), there are many options for bivariate copulas. This motivates pair-copula constructions (PCCs) (Aas & Berg, 2009; Brechmann & Schepsmeier, 2013; Kurowicka & Cooke, 2007). The basic idea of the PCCs is to decompose the d-dimensional multivariate density into $d(d-1)/2$ pair-copula densities or building blocks that can provide a flexible approach for modeling multivariate distributions of any dimension (Bedford & Cooke, 2002; Joe 1996, 1997; Schirmacher & Schirmacher, 2008). In order to systemize PCCs,

Table 2
Analogous to Table 1 but for El Niño and Global Temperature

Distributions	El Niño	Temperature	Runoff	Precipitation
Normal	2.62	0.91	5.02	0.89
Gamma	2.50	0.87	4.51	0.83
Lognormal	**2.44**	**0.86**	**4.32**	**0.82**
Weibull	5.61	2.13	7.29	1.49

Note. The best distribution for each variable is indicated in bold.

Bedford and Cooke (2001, 2002) introduced tree representations, called regular vines. Two subsets of regular vines are commonly in use: canonical vines (C-vines) and drawable vines (D-vines). Here we use C-vines to identify different decompositions of PCCs. Figure 2 is a graphical representation of three-dimensional (Figure 2a) and four-dimensional (Figure 2b) C-vines employed herein. It was constructed by choosing a specific order of variables and consists of $n-1$ linked trees T_i, $i=1,\ldots,n-1$. The order defines the sequence of conditioning in the PCCs: first variable 1 is conditioned, then variable 2 and so on (Brechmann & Schepsmeier, 2013). For instance, at T_1 in Figure 2a, the circled nodes represent the three marginal density functions of El Niño (or La Niña or ENSO neutral states), precipitation and surface runoff (also see Figure 2c).

Each edge is labeled and modeled with the pair-copula of the variables that it represents. The edges in level i become nodes for the next level $i+1$. A n-dimensional density of the C-vine copula is expressed as (Czado et al., 2012):

$$f(x_1,\ldots,x_n)=\prod_{k=1}^{n} f_k(x_k)\times\prod_{i=1}^{n-1}\prod_{j=1}^{n-i} c_{i,i+j|1:(i-1)}\left(F(x_i|x_1,\ldots,x_{i-1}),F(x_{i+j}|x_1,\ldots,x_{i-1})\right) \tag{3}$$

Here $f(x_1,\ldots,x_n)$ is the joint density function of n-dimensional random variables, $f_k(x_k)$ ($k=1,\ldots,n$) denotes the n marginal densities, and $c_{i,i+j|1:(i-1)}$ represents the bivariate copula densities. We give orders of the four variables examined herein, such as (x_1, x_2, x_3, x_4) representing variables (ENSO, global temperature, runoff, precipitation), thus the employed three-dimensional and four-dimensional density functions can be specified as:

$$f_{134}=f_1\cdot f_3\cdot f_4\cdot c_{14}\cdot c_{13}\cdot c_{43|1} \tag{4}$$

$$f_{1234}=f_1\cdot f_2\cdot f_3\cdot f_4\cdot c_{12}\cdot c_{13}\cdot c_{14}\cdot c_{23|1}\cdot c_{24|1}\cdot c_{34|21} \tag{5}$$

where x_1 is the condition in the three-dimensional vine copula and (x_1, x_2) is the joint condition in the four-dimensional case, whose coupling strength will be taken into account in order to determine their mutual effects on the response variables.

As mentioned before, a large number of bivariate copulas are available for building pair-copulas of the PCCs to realize a wide range of dependence structures. Five widely applied bivariate copulas (Gaussian, t,

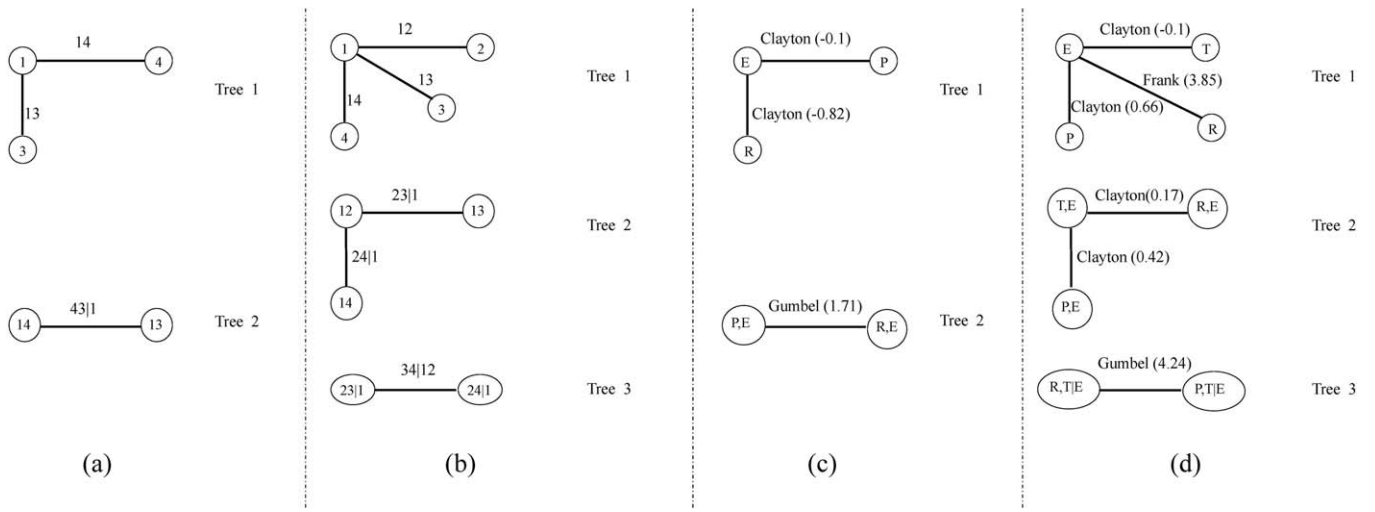


Figure 2. Tree representation of the (a) three-dimensional and (b) four-dimensional C-vine copula. Climate variables corresponding to the root nodes in (c) three-dimensional and (d) four-dimensional C-vine copula. E, P, R, T are short for ENSO states, precipitation, surface runoff, and the global averaged temperature, respectively. The fitted bivariate copula and its dependence parameter are provided for each pair of variables at the root nodes in Climate Division 5 as an example.

Gumbel, Frank, and Clayton) are examined herein. We select the bivariate copula suitable for each pair of variables based on Akaike information criterion (AIC) following Schepsmeier et al. (2012). The distribution functions of the five bivariate copulas are included in the supporting information.

A remaining part of completing the C-vine copula relates to the conditional distribution function, i.e., $F(x|v)$, where v denotes a vector of r-dimensional variables. For a pair-copula term in tree $r+1$, this can be inferred using the pair-copula of the previous trees $1, \ldots, r$ by sequentially applying the formula below:

$$h(x, v, \theta) := F(x|v) = \frac{\partial C_{xv_j|v_{-j}}\left(F\left(x|v_{-j}\right), F\left(v_j|v_{-j}\right)|\theta\right)}{\partial F\left(v_j|v_{-j}\right)} \tag{6}$$

where v_j is an arbitrary component of v; v_{-j} denotes the vector v but excluding the jth component v_j; and $C_{xv_j|v_{-j}}$ is a bivariate copula distribution function with parameter(s) θ specified in tree r. The notion of h-function is introduced as the conditional distribution function, and its analytical expression for the pair-copula is derived by Schirmacher and Schirmacher (2008) and Aas et al. (2009). We also included the conditional distribution functions of five bivariate copulas in Supplementary Materials.

2.2.3. Conditional Simulations via Vine Copula

To generate simulations from the conditional states of vine copula, the inverse forms of h-functions are applied. Referring to our three-dimensional case, phases of ENSO signal are considered the only factor that conditions the joint distribution of precipitation and surface runoff. For instance, assume El Niño (x_1) and precipitation (x_4) have uniform margins of u_1 and u_4, respectively. With a given conditional distribution function of u_1 and u_4, i.e., $h(u_4|u_1, \theta)$, we aim to simulate u_4 based on the information of u_1 using the conditional copula. We first generate random samples, e.g., $\tau = 0.01, 0.1, \ldots, 0.99$ which can be regarded as a random probability level of the conditional cumulative distribution functions. For a fixed probability τ, we infer u_4 from $C_{u_4|u_1}$ using $u_1 = C^{-1}_{u_4|u_1}(\tau|u_2, \theta) = h^{-1}(\tau|u_1, \theta)$, where $C^{-1}_{u_4|u_1}$ is the inverse of the copula function known as the τ quantile curve of the copula (Min & Czado, 2010; Schirmacher & Schirmacher, 2008). Simulations of precipitation can be estimated based on the τth copula-based conditional quantile function, i.e., $h^{-1}(\tau|u_1, \theta)$ as follows:

$$x_4 = F^{-1}\left[h^{-1}(\tau|u_1, \theta_{14})\right] \tag{7}$$

where θ_{14} represents the dependence parameter of the joint distribution of (x_1, x_4). Note that we also examine when the condition, i.e., (x_1) is replaced by La Niña and ENSO neutral states, respectively.

In our four-dimensional scenario, the compound floods consist of precipitation (x_4) and surface runoff (x_3) with conditions of both El Niño (x_1) and global temperature (x_2). To examine joint effects of ENSO and temperature conditions on precipitation, the inverse forms of h-functions regarding a four-dimensional C-vine structure are sequentially applied as in:

$$x_4 = F^{-1}\left\{h^{-1}\left[\left(h^{-1}\left(\tau|h(u_2|u_1, \theta_{12}), \theta_{24|1}\right)\right)|u_1, \theta_{14}\right]\right\} \tag{8}$$

where θ_{12} identifies the dependency of the joint distribution of underlying conditions (x_1, x_2), which can be interpreted as an indicator for measuring the mutual interaction between the two conditions; and θ_{14}, $\theta_{24|1}$ denote the parameters of c_{14}, $c_{24|1}$, respectively.

First, we generate a sample size of 500 uniformly distributed random values over the interval [0, 1] (i.e., the τ value) using Monte Carlo simulations. Equations (7) and (8) are then applied to calculate the 500 realizations (simulations) of precipitation under the individual condition of El Niño (analogous for La Niña and ENSO neutral conditions), and under the joint conditions of El Niño and global averaged temperature, respectively. In a similar way, we can derive simulations of surface runoff with the given climatic conditions. The inverse forms of the five candidate copulas are provided in the supporting information.

3. Results

3.1. Model Validation

Figures 2c and 2d show the C-vine structure with climate variables of interest at the root nodes. Specifically, the three-dimensional C-vine copula (Figure 2c) models the combination of standardized precipitation (P) and surface runoff (R) anomalies with ENSO states (E) as the underlying condition. Since we diagnose separate

effects of El Niño, La Niña, and ENSO neutral tropical Pacific states on the joint distribution of precipitation and surface runoff, the notation of E denotes the three individual ENSO states. Heuristically, the dependence of TX floods on ENSO states is implicitly controlled by the conditional structure, i.e., (23|1), thereby allowing us to evaluate how surface runoff and precipitation can be modulated by ENSO conditions. The conditional

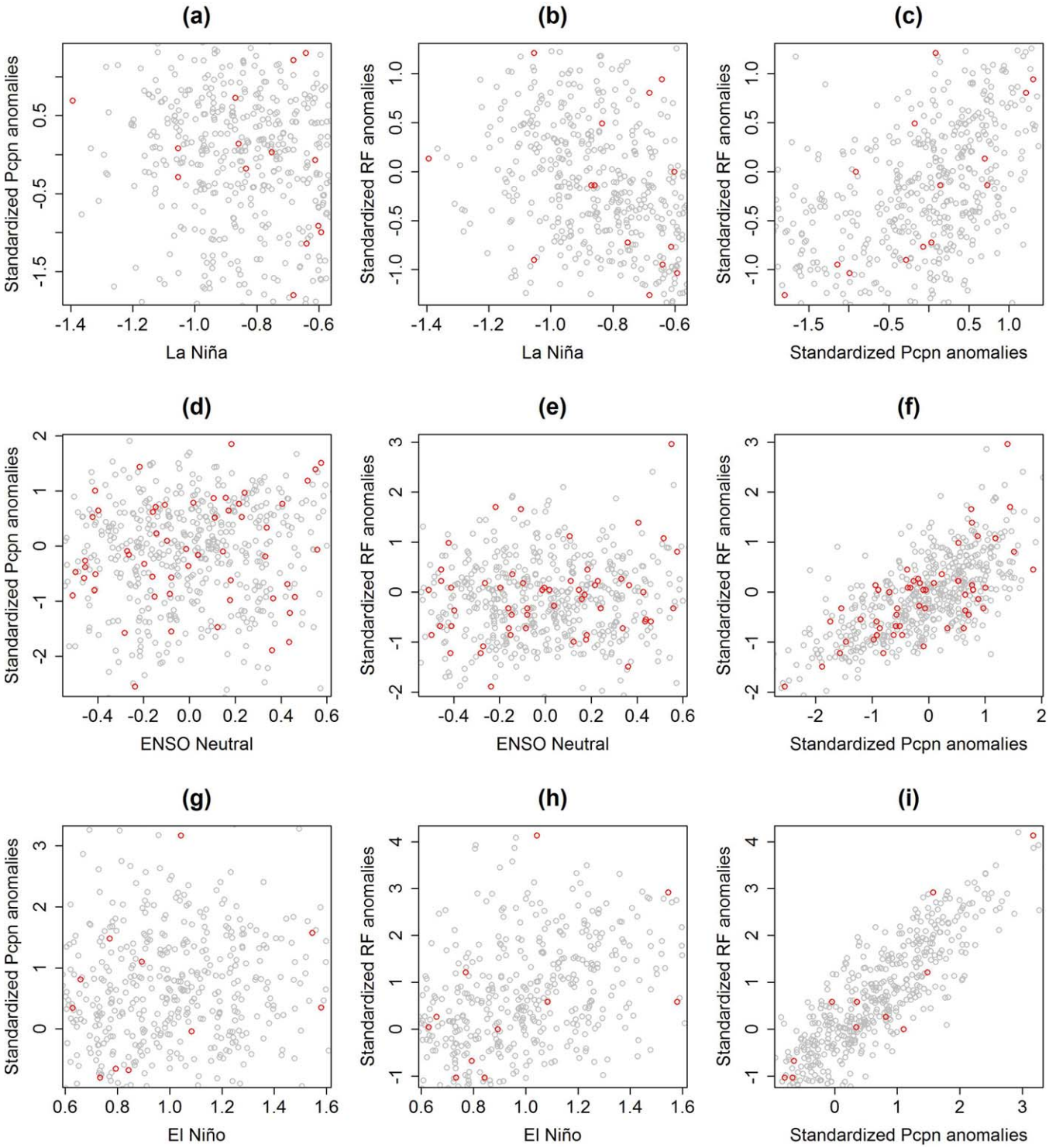


Figure 3. Five hundred random samples (gray circles) generated from the fitted three-dimensional vine copulas are validated against the observations (red circles) in pair at Climate Division 5. Pcpn is short for Precipitation and RF is short for runoff.

strength of rising temperature (T in Figure 2d) is examined in the four-dimensional analysis following the decomposition shown in Figure 2d. We give bivariate copula with inferred dependence parameters for constructing joint distribution of variables at Climate Division 5 (D5) as an example.

We generate 500 simulations of each variable from the fitted pair-copula to offer a visual goodness of fit test at D5. In Figure 3, simulations (gray circles) are validated against the observed (red circles) for each pair of variables related to El Niño (first row), La Niña (second row), and ENSO neutral (bottom row) states, respectively. It is clear that the random generations provide good coverage of the observations in each subplot, including the upper and lower tail events with respect to the individual variable. In addition to the agreement in the variability of univariables, the covariability of the simulated and the observed pairs is largely consistent, showing that the fitted vine copula has characterized a realistic interdependence between attending physical processes with suitable marginal distributions.

Validation is conducted for the rest of the climate divisions. The results attest to the goodness of fit of both bivariate copula and marginal distribution applied to each climate division (not shown for sake of brevity). These diagnoses build confidence in the robustness of our approach for examining the response of combinations of extreme events to underlying conditions in the subsequent analysis.

3.2. Individual Effect of ENSO States on TX Compound Floods

We first estimated the joint distribution of standardized precipitation and surface runoff anomalies conditioned by individual ENSO states. Five hundred simulations of precipitation and surface runoff in response

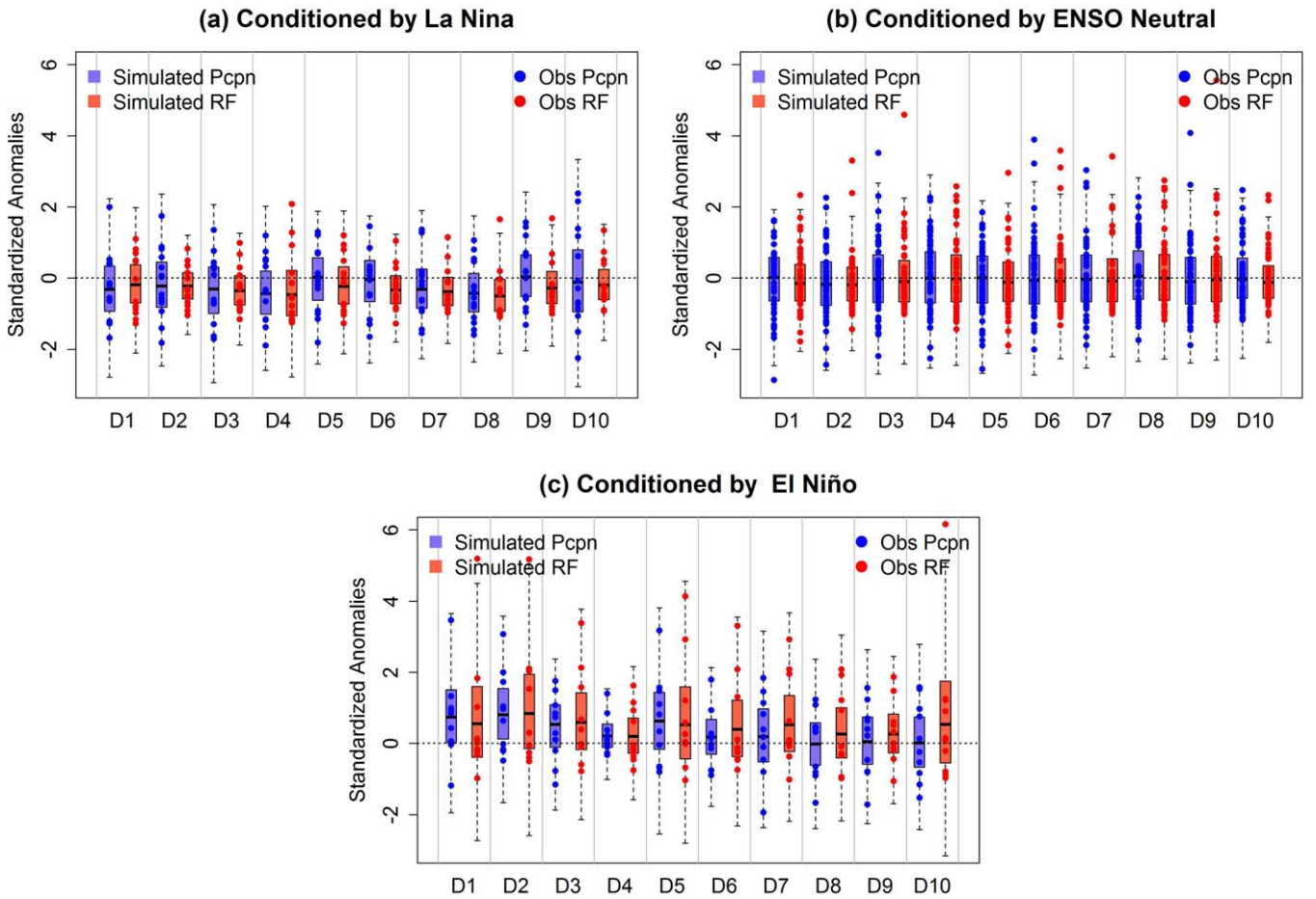


Figure 4. Boxplots for simulations of precipitation (blue boxes) and surface runoff (red boxes) conditioned by (a) La Nina, (b) ENSO Neutral, and (c) El Niño states at the 10 climate divisions. The observed precipitation (blue dots) and runoff (red dots) composites corresponding to the three ENSO conditions are plotted for validation. Precipitation and surface runoff are standardized anomalies relative to the May–August climatology of 1932–2011 (black dash line). Pcpn is short for Precipitation and RF is short for runoff.

to the given ENSO state were generated and displayed in a box-whisker plot. Figure 4 summarizes the simulations of historical May–August averaged precipitation (blue box) and surface runoff (red box) corresponding to La Niña (Figure 4a), ENSO neutral (Figure 4b), and El Niño (Figure 4c) states in the 10 climate divisions. To validate our conditional framework, we sampled the precipitation (blue dots) and runoff (red dots) observed under each scenario. A quick comparison shows the simulations are qualitatively consistent with those from observations, though with some extreme wet cases falling beyond the upper 2.5% quantile of the box-whisker estimates, mostly associated with the ENSO neutral state. By examining the climate-division-based results, it is fair to say that the spatial variation of precipitation and runoff has been reasonably described by conditioning upon the ENSO effect in the sense that the probability space of the observed bivariates fall within the range of the model's simulations across the region. Warranted by large sample sizes and by evidence that the conditional framework produces realistic statistics of both rainfall and surface runoff, we can evaluate how the underlying conditions affect the compound floods with more reliability.

Differences in the response of precipitation and runoff to the three ENSO states are noticeable with respect to the median of the box-whisker simulations. With the presence of La Niña (Figure 4a), the median values of all the distributions are below the climatology (black dash line) of May–August. Although the ENSO neutral state shows a slight increase, neither precipitation nor runoff is likely to have a median exceeding the

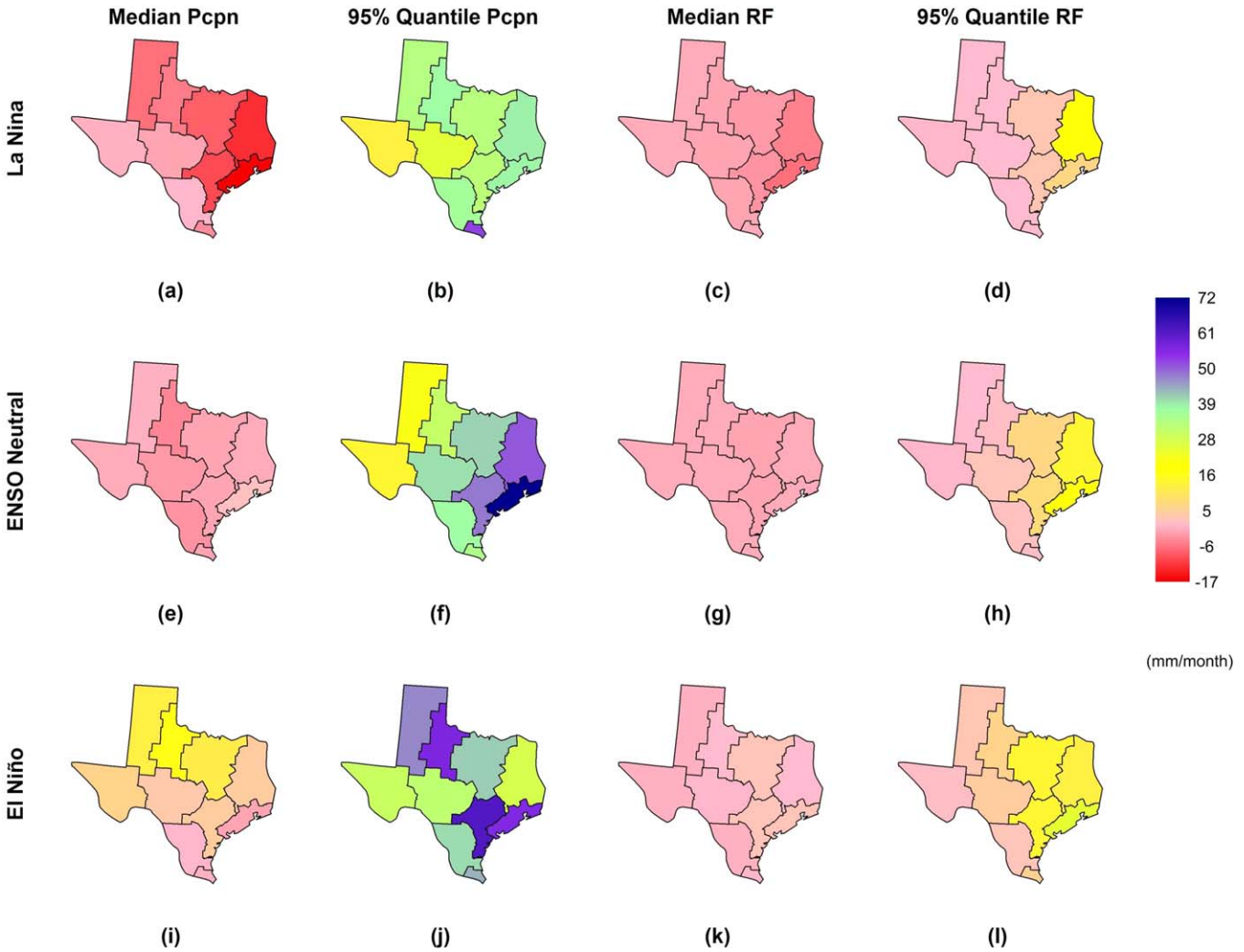


Figure 5. Spatial map based upon simulations of median and 95% quantile of precipitation anomalies (left two columns in mm/month) and runoff anomalies (right two columns in mm/month) corresponding to La Nina (top), ENSO Neutral (middle), El Nino states (bottom). Precipitation and runoff anomalies are calculated with respect to the 1932–2011 climatology of May–August. Precipitation is short as Pcpn and runoff is short as RF.

long-term mean. Both scenarios dictate a low likelihood of severe compound floods in the 10 climate divisions. The effect on precipitation and runoff is opposite under the condition of El Niño (Figure 4c). In addition to increases in the median of El Niño-related box-whisker plots, our analysis indicates the extreme magnitude of rainfall and runoff (as large as exceeding three standard deviations) to be irreconcilable with either La Niña or ENSO neutral states. The results affirm El Niño to be a more favorable condition for strengthening both the mean and extreme states of precipitation and runoff over TX. With increased mean and extreme values, our results indicate an enhanced likelihood of compound floods that can result from the interplay of individually nonextreme precipitation and runoff variables during the El Niño condition.

To have a spatial view of changes in the variables under given conditions, Figure 5 collects the results of 10 climate divisions. We show the median (upper two rows) and 95% quantile (bottom two rows) of precipitation (left two columns) and runoff (right two columns) anomalies for the three ENSO states (also see supporting information Table S1). Consistent with the estimates using standardized anomalies in Figure 4, the conditionality of May–August rainfall is pronounced with El Niño, though not uniform in space. The largest increases occur in D1, 2, and 7, where the median has exceeded the seasonal climatology by 5–16 mm/month (Figure 5i) with extreme cases reaching an exceedance of 60 mm/month (Figure 5j). This is also the case for surface runoff, showing moderate increases overall, with a notable increase in D7 and 8 (Figure 5l). Increases in extreme anomalies of precipitation and surface runoff affect occurrences of extreme compound floods, particularly under El Niño conditions. By contrast, the other two ENSO phases induce 2–4 times less seasonal rainfall and runoff over the region. In summary, TX compound floods show more sensitivity to the

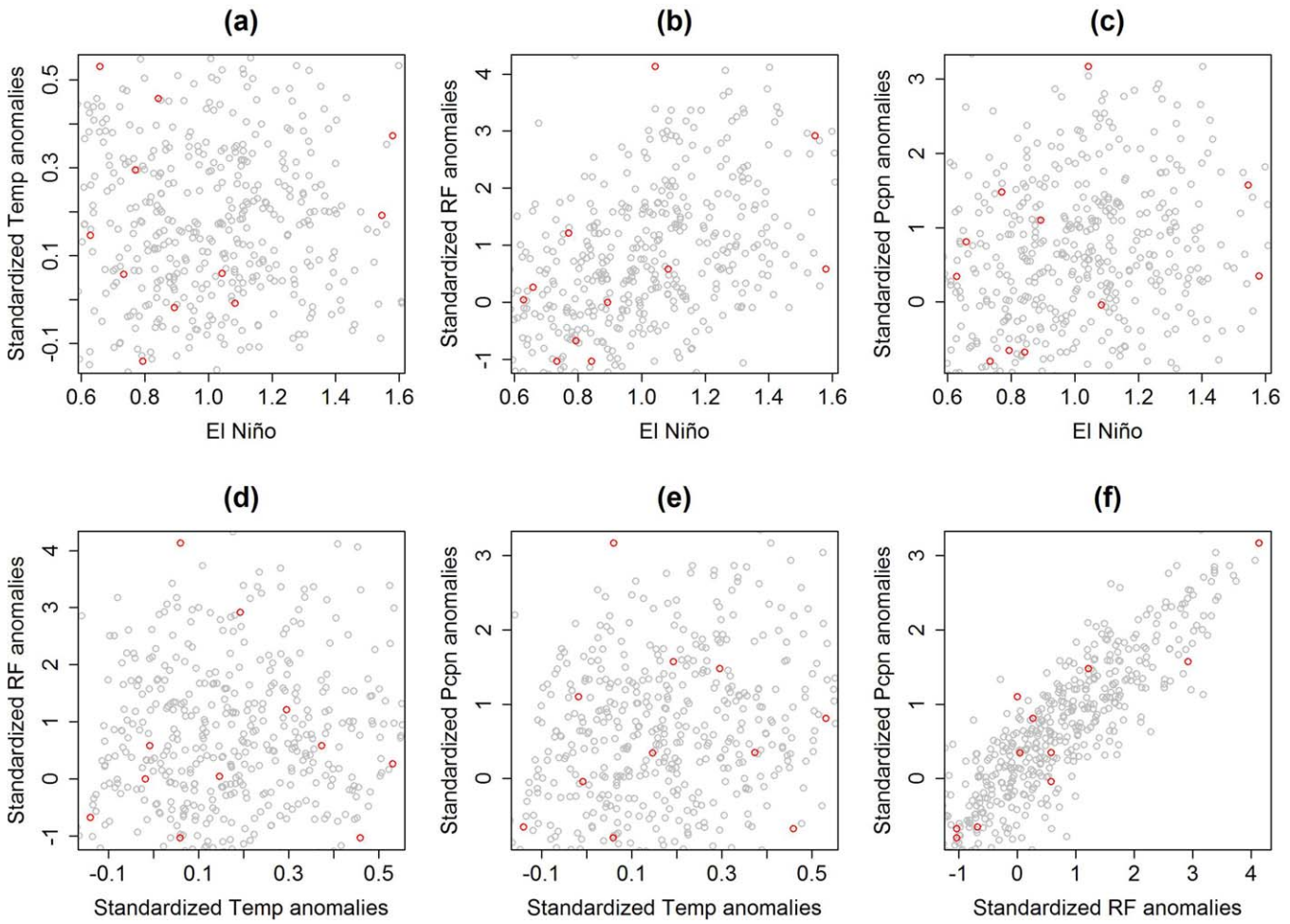


Figure 6. Five hundred random samples (gray circles) generated from the fitted four-dimensional vine copulas are validated against the observations (red circles) in pair at Climate Division 5. Pcpn is short for Precipitation. RF is short for runoff. Temp is short for global averaged temperature.

presence of El Niño, a symptom of increases in both precipitation and surface runoff, thereby yielding an enhanced likelihood of compound floods in TX during May–August.

3.3. Combined Effects of El Niño and Rising Global Temperature on TX Compound Floods

Another purpose of this study is to examine changes in the combination of extreme events caused by the mutual interaction of underlying conditions. El Niño has been identified as a strong factor in conditioning TX May–August compound floods. We next incoporated both global temperature and El Niño to condition the compound floods. Our four-dimensional analysis consists of precipitation and surface runoff conditional upon global averaged temperatures and El Niño during the wet season. Analogous to Figure 3, we present a scatter plot for visualizing goodness of fit of the four-dimensional vine copula at D5 as an example (see Figure 6). The bivariate copula fitted to each pair of variables can be viewed in Figure 2d. Again, 500 simulations (gray circles) were derived for each variable and validated against observations (red circles) in pairs. This result, in addition to the pair-relationship in Figure 3, shows an agreement regarding the simulated and observed relationships of global temperature with the rest of the variables, i.e., rainfall, runoff, and El Niño. By building a connection to global temperature, it becomes feasible to diagnose the jointly conditional effects of warming and El Niño on TX compound floods in a quantitative manner.

To illustrate, we examined two scenarios created by varying the magnitude of the global temperature. One scenario was conditioned by El Niño and temperatures with a magnitude between the 30% and 70% quantiles of global averaged temperature, which is about 0.06–0.15°C above its long-term mean. The joint

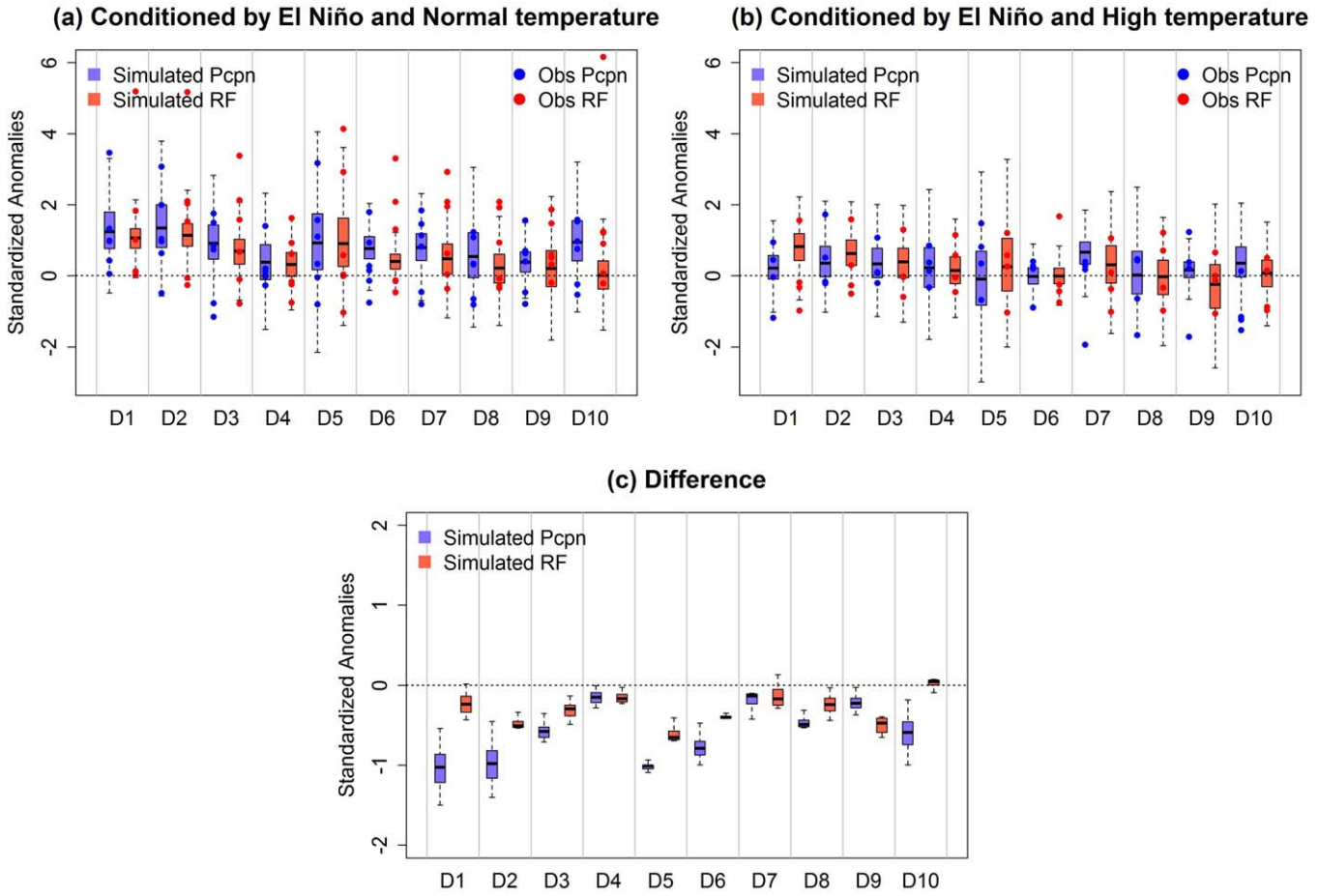


Figure 7. Boxplots for simulations of precipitation (blue box) and runoff (red box) under the joint condition of El Niño and Normal temperature (30–70% quantile of the global averaged temperature) (a), and under the joint condition of El Niño and High temperature (above 70% quantile of the global averaged temperature) (b) at the 10 climate division. The difference between (b) and (a) is placed in plot (c). The observed precipitation (blue dots) and runoff (red dots) composites corresponding to each scenario are plotted for validation. Precipitation and runoff are standardized anomalies relative to the 1932–2011 climatology of May–August (black dash line). Pcpn is short for Precipitation and RF is short for runoff.

condition of the other scenario involves El Niño and temperatures exceeding the 70% quantile, i.e., 0.3–0.5°C higher than the climatology. The temperature condition in the first scenario can be interpreted as an analogy to the historical temperature state of the wet season from 1932 to 1950 (hereafter, Normal temp). The condition in the second scenario is analogous to a warmer globe during 1950–2011 (hereafter, High temp). With the specified conditions, large simulations of precipitation and surface runoff were generated using the conditional copula to facilitate the examination of changes in compound floods.

Figure 7 shows the standardized anomalies of precipitation (blue box) and surface runoff (red box) simulated under the joint condition of El Niño and Normal Temp (Figure 7a) as well as the joint condition of El Niño and High Temp (Figure 7b) at the 10 climate divisions. Simulations from the conditional vine copula were validated against observed precipitation (blue dots) and runoff (red dots) for the two scenarios distinguished by different global temperatures. Akin to the previous assessment, the simulated results are largely in agreement with the observations, attesting to the suitability of our approach for modeling conditional distribution and spatial distribution of TX compound floods. Nevertheless, by visual comparison, the box-whisker estimates of the two scenarios quite resemble each other. We made another panel (Figure 7c) showing the difference between plots (b) and (a), in which the result reveals a slight decrease in El Niño-related precipitation and surface runoff anomalies across TX when the global temperature increases. Our

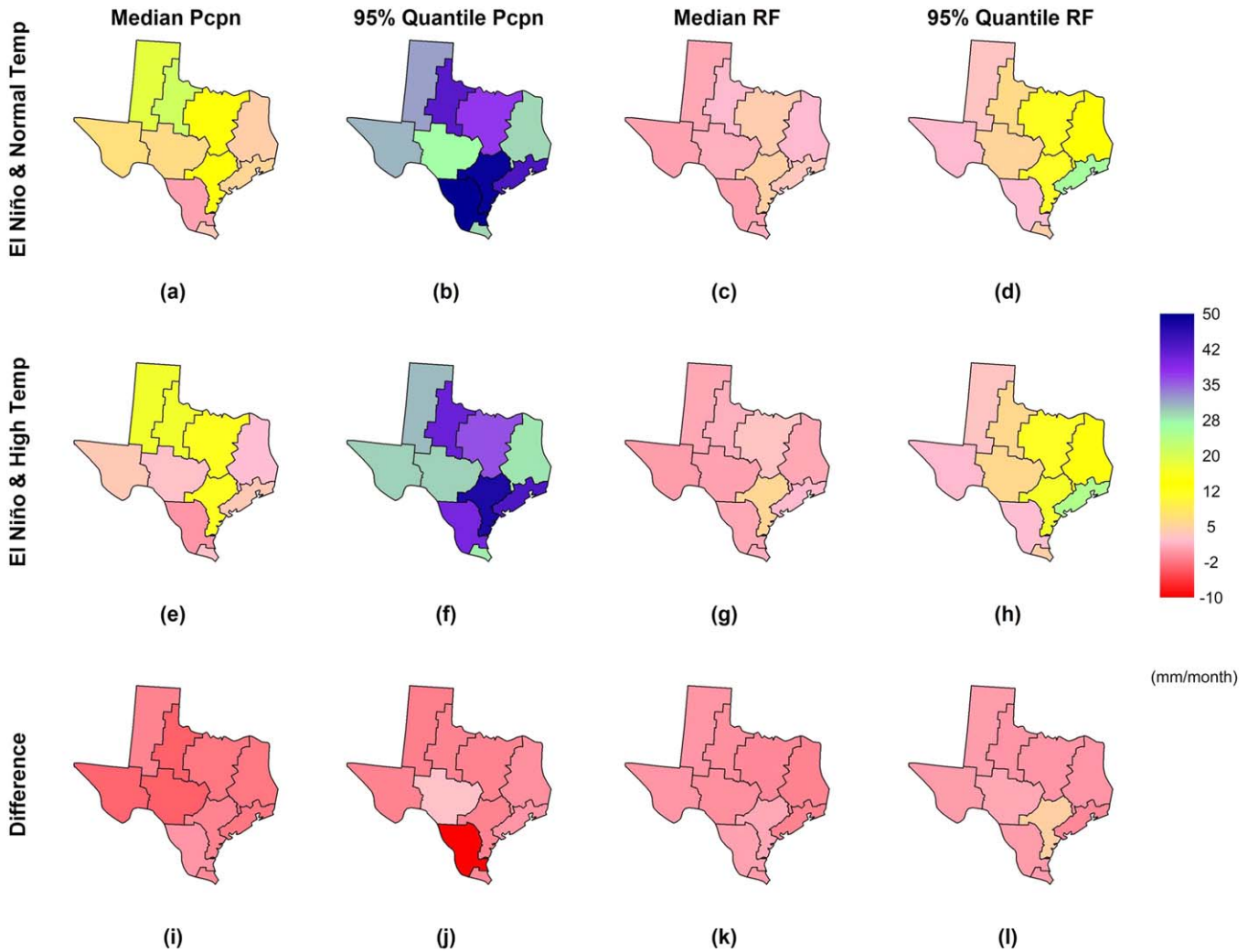


Figure 8. Spatial map based upon simulations of median and 95% quantile of precipitation anomalies (left two columns in mm/month) and runoff anomalies (right two columns in mm/month) under the joint condition of El Niño and Normal temperature (top), and under the joint condition of El Niño and High temperature (middle). The difference between the second and the first row is placed in the bottom row. Precipitation and runoff anomalies are calculated with respect to the 1932–2011 climatology of May–August. Pcpn is short for Precipitation and RF is short for runoff.

result is also supported by Sillmann et al. (2013) who examined changes in precipitation-based indices on global and regional scales using different emission scenarios in the Coupled Model Intercomparison Project Phase 3 and Phase 5 multimodel ensembles. Their result indicates a slight decrease in the projected maximum 5 day precipitation of 2081–2100 relative to the reference period 1981–2000 over central North America during the summer season under scenarios of higher greenhouse gas emissions.

We also produced a spatial map based on the precipitation and runoff estimates of the two scenarios (Figure 8). The median and 95% quantile of precipitation (left two columns) and runoff anomalies (right two columns) are presented (also see supporting information Table S2), based on which we calculate the difference between the first (top row) and second scenario (second row) (bottom row). In accordance with the findings in Figure 7, the comparison shows that the severity of El Niño-related rainfall and runoff over TX has been slightly reduced by approximately 2 mm/month of precipitation and 0.5 mm/month of runoff averaged over the 10 divisions under the condition of high global temperature. This reduction is consistent with the trend of precipitation and surface runoff composites under given conditions, while no significant changes are found to suggest a different interrelationship between the two conditioning factors. Nor were there material changes in the mutual effect of El Niño and temperatures on TX compound floods in a warmer world.

4. Discussion and Conclusions

Among challenges concerning compound events, the IPCC report highlights a need to better understand cases that involve mutual interaction between climate processes, which can either lead to a damping or enhancement of the event impacts (Field et al., 2012). The current study has presented a conditional framework of vine copula for assessing compound events with underlying conditions that may amplify the compounding effects. Following the IPCC's definition, our TX compound floods involve a combination of heavy precipitation and large surface runoff, associated with underlying conditions of ENSO forcing and rising global temperatures. We illustrate this framework by examining (1) the individual effect of ENSO intensities, and (2) the joint effects of El Niño and extreme global temperature on compound floods in TX.

Our diagnosis first demonstrated that the selected three-dimensional and four-dimensional vine copula can well represent the interrelationship between observed variables. The covariability of each pair of variables simulated by the fitted vine copula therefore displayed a consistent pattern with observations. Reliant upon the conditional formulism of fitted vine copulas, simulations of precipitation and surface runoff can be derived under the condition of ENSO states alone, and under the joint condition of El Niño and global temperature, respectively. For both conditional diagnoses, the simulated distribution of precipitation and surface runoff were in agreement with observations. The result provides evidence that the conditional framework characterized a realistic relationship between variables and underlying conditions as well as between the underlying conditions themselves, therefore rendering robustness in examining the response of compound events to physical processes.

A stronger dependence of TX rainfall and runoff on El Niño during May–August was revealed when examining the three individual ENSO states as conditions. Analysis of the 10 climate divisions shows that both the mean and extreme states of precipitation and runoff have increased by concurrent El Niño forcing, while the median of rainfall and runoff simulations related to La Niña (ENSO neutral) remained below (close to) their climatology. The results, consistent with previous findings attest to the conditional strength of El Niño in enhancing the intensity and likelihood of TX compound floods. To the extent that global surface temperature is closely associated with El Niño and precipitation, the interdependence between El Niño and rising global temperature was addressed in order to determine their combined effects on TX floods. We found that El Niño-induced enhancement was not appreciably different under the presence of a warming signal, thereby indicating a similar mutual effect of El Niño and global temperature on TX compound floods in a warmer world.

By regarding underlying factors as conditional states using vine copula, the conditional framework of vine copula demonstrates capability in yielding predictive information of compound events by leveraging a realistic connection to their physical drivers. While having applied an effective approach to quantify changes in extreme events, our analysis of TX flooding did not just target the extreme tail of the involved variables. Rather, we examined cases in which combinations of rainfall and surface runoff that were not themselves extremes could lead to an extreme flooding when combined. In this sense, the response of extreme tail

variables may differ from that which is implied by the current result which includes variables not extreme enough to reflect the effect of tail (in)dependence. Also, in the observational data, our sample size corresponding to the given conditions is limited. To reduce the uncertainty in the statistical simulations, large ensembles of climate model simulations are desired.

We note that our study only examined one factor (rising global temperature) relevant to understanding global warming on El Niño and precipitation; other plausible factors are yet to be incorporated in a comprehensive assessment. To this point, it would be more reasonable to interpret the current study as a proxy for examining the sensitivity of compound TX floods to a certain warming condition rather than an attribution study of TX floods to human-induced climate change. We also note that our conclusions are representative of floods occurring in the months of May–August, and in the TX region only. Findings and results may vary in other regions and other seasons. To examine whether there are changes in El Niño dynamics and in its associated atmospheric circulation as a result of the mutual effect is beyond the capability of our statistical framework because it would require large ensemble climate simulations. The emphasis is that the proposed framework can be applied to diagnose underlying conditions of extreme events including not only climatic factors but also many other human activity-related factors, such as land-use change, the construction of dams, etc.

Acknowledgments
The precipitation and surface runoff of Texas are available from the website of Climate Prediction Center (CPC): ftp://ftp.cpc.ncep.noaa.gov/wd51yf/us.m. Global temperature is available from Met Office Hadley Centre observations data sets http://www.metoffice.gov.uk/hadobs/index.html. The C-vine copula was selected using the RVineCopSelect function in the VineCopula package in R. The first and the last authors acknowledge partial support from National Key R&D Program of China (2017YFC0405900) and National Natural Science Foundation of China (grants 91547202; 51779279). The fourth author acknowledges support from NASA Minority University Research and Education Project (MUREP) Institutional Research Opportunity grant (NNX15AQ06A). All the authors appreciate the constructive comments and suggestions of the editors and the three anonymous reviewers.

References

Aas, K., & Berg, D. (2009). Models for construction of multivariate dependence—A comparison study. *The European Journal of Finance*, *15*(7–8), 639–659. https://doi.org/10.1080/13518470802588767

Aas, K., Czado, C., Frigessi, A., & Bakken, H. (2009). Pair-copula constructions of multiple dependence. *Insurance: Mathematics and Economics*, *44*(2), 182–198.

Adler, R. F., Gu, G., Wang, J. J., Huffman, G. J., Curtis, S., & Bolvin, D. (2008). Relationships between global precipitation and surface temperature on interannual and longer timescales (1979–2006). *Journal of Geophysical Research*, *113*, D22104. https://doi.org/10.1029/2008JD010536

Allan, R. P., & Soden, B. J. (2008). Atmospheric warming and the amplification of precipitation extremes. *Science*, *321*(5895), 1481–1484. https://doi.org/10.1126/science.1160787

Bedford, T., & Cooke, R. M. (2001). Probability density decomposition for conditionally dependent random variables modeled by vines. *Annals of Mathematics and Artificial Intelligence*, *32*(1–4), 245–268. https://doi.org/10.1023/A:1016725902970

Bedford, T., & Cooke, R. M. (2002). Vines: A new graphical model for dependent random variables. *Annals of Statistics*, 1031–1068. https://doi.org/10.1214/aos/1031689016

Bevacqua, E., Maraun, D., Haff, I. H., Widmann, M., & Vrac, M. (2017). Multivariate statistical modelling of compound events via pair-copula constructions: Analysis of floods in Ravenna (Italy). *Hydrology and Earth System Sciences*, *21*(6), 2701–2723. https://doi.org/10.5194/hess-21-2701-2017

Brechmann, E. C., & Schepsmeier, U. (2013). Modeling dependence with C-and D-vine copulas: The R-package CDVine. *Journal of Statistical Software*, *52*(3), 1–27. https://doi.org/10.18637/jss.v052.i03

Cai, W., Santoso, A., Wang, G., Yeh, S. W., An, S. I., Cobb, K. M., et al. (2015). ENSO and greenhouse warming. *Nature Climate Change*, *5*(9), 849–859. https://doi.org/10.1038/nclimate2743

Chebana, F., & Ouarda, T. B. (2011). Multivariate quantiles in hydrological frequency analysis. *Environmetrics*, *22*(1), 63–78. https://doi.org/10.1002/env.1027

Cheng, L., Hoerling, M., AghaKouchak, A., Livneh, B., Quan, X. W., & Eischeid, J. (2016). How has human-induced climate change affected California drought risk?. *Journal of Climate*, *29*(1), 111–120. https://doi.org/10.1175/JCLI-D-15-0260.1

Church, J. A., & White, N. J. (2006). A 20th century acceleration in global sea-level rise. *Geophysical Research Letters*, *33*, L01602. https://doi.org/10.1029/2005GL024826

Climate Prediction Center (2015). Keep calm and stop obsessing over weekly changes in ENSO. Retrieved from https://www.climate.gov/news-features/blogs/enso/keep-calm-and-stop-obsessing-over-weekly-changes-enso

Collins, M., An, S. I., Cai, W., Ganachaud, A., Guilyardi, E., Jin, F. F., et al. (2010). The impact of global warming on the tropical Pacific Ocean and El Niño. *Nature Geoscience*, *3*(6), 391–397. https://doi.org/10.1038/ngeo868

Czado, C., Schepsmeier, U., & Min, A. (2012). Maximum likelihood estimation of mixed C-vines with application to exchange rates. *Statistical Modelling*, *12*(3), 229–255. https://doi.org/10.1177/1471082X1101200302

De Michele, C., & Salvadori, G. (2003). A generalized Pareto intensity-duration model of storm rainfall exploiting 2-copulas. *Journal of Geophysical Research*, *108*(D2), 4067. https://doi.org/10.1029/2002JD002534

Dole, R., Hoerling, M., Perlwitz, J., Eischeid, J., Pegion, P., Zhang, T., et al. (2011). Was there a basis for anticipating the 2010 Russian heat wave?. *Geophysical Research Letters*, *38*, L06702. https://doi.org/10.1029/2010GL046582

Favre, A. C., El Adlouni, S., Perreault, L., Thiémonge, N., & Bobée, B. (2004). Multivariate hydrological frequency analysis using copulas. *Water Resources Research*, *40*, W01101. https://doi.org/10.1029/2003WR002456

Field, C. B., Barros, V., Stocker, T. F., Qin, D., Dokken, D. J., Ebi, K. L., et al. (Eds.) (2012). *Managing the risks of extreme events and disasters to advance climate change adaption, A special report of working groups I and II of the intergovernmental panel on climate change*, Cambridge, UK: Cambridge University Press.

Fischer, E. M., Seneviratne, S. I., Lüthi, D., & Schär, C. (2007). Contribution of land-atmosphere coupling to recent European summer heat waves. *Geophysical Research Letters*, *34*, L06707. https://doi.org/10.1029/2006GL029068

Gershunov, A. (1998). ENSO influence on intraseasonal extreme rainfall and temperature frequencies in the contiguous United States: Implications for long-range predictability. *Journal of Climate*, *11*(12), 3192–3203. https://doi.org/10.1175/1520-0442(1998)011<3192:EIOIER>2.0.CO;2

Gershunov, A., & Barnett, T. P. (1998). ENSO influence on intraseasonal extreme rainfall and temperature frequencies in the contiguous United States: Observations and model results. *Journal of Climate*, *11*(7), 1575–1586. https://doi.org/10.1175/1520-0442(1998)011<1575:EIOIER>2.0.CO;2

Hao, Z., & Singh, V. P. (2013). Modeling multi-site streamflow dependence with maximum entropy copula. *Water Resources Research*, *49*, 7139–7143. https://doi.org/10.1002/wrcr.20523

Hao, Z., & Singh, V. P. (2016). Review of dependence modeling in hydrology and water resources. *Progress in Physical Geography*, *40*(4), 549–578. https://doi.org/10.1177/0309133316632460

Heffernan, J. E., & Tawn, J. A. (2004). A conditional approach for multivariate extreme values (with discussion). *Journal of the Royal Statistical Society: Series B (Statistical Methodology)*, *66*(3), 497–546. https://doi.org/10.1111/j.1467-9868.2004.02050.x

Hendon, H. H. (2003). Indonesian rainfall variability: Impacts of ENSO and local air-sea interaction. *Journal of Climate*, *16*(11), 1775–1790. https://doi.org/10.1175/1520-0442(2003)016<1775:IRVIOE>2.0.CO;2

Hoell, A., Hoerling, M., Eischeid, J., Wolter, K., Dole, R., Perlwitz, J., e al. (2015). Does El Niño intensity matter for California precipitation?. *Geophysical Research Letters*, *43*, 819–825. https://doi.org/10.1002/2015GL067102

Horel, J. D., & Wallace, J. M. (1981). Planetary-scale atmospheric phenomena associated with the Southern Oscillation. *Monthly Weather Review*, *109*(4), 813–829. https://doi.org/10.1175/1520-0493(1981)109<0813:PSAPAW>2.0.CO;2

Hoskins, B. J., & Karoly, D. J. (1981). The steady linear response of a spherical atmosphere to thermal and orographic forcing. *Journal of Atmospheric Sciences*, *38*(6), 1179–1196. https://doi.org/10.1175/1520-0469(1981)038<1179:TSLROA>2.0.CO;2

Huang, J., van den Dool, H. M., & Georgarakos, K. P. (1996). Analysis of model-calculated soil moisture over the United States (1931–1993) and applications to long-range temperature forecasts. *Journal of Climate*, *9*, 1350–1362. https://doi.org/10.1175/1520-0442(1996)009<1350:AOMCSM>2.0.CO;2

Joe, H. (1996). Families of m-variate distributions with given margins and m (m-1)/2 bivariate dependence parameters. In L. Rüschendorf, B. Schweizer, & M.D. Taylor (Eds.), *Distributions with fixed marginals and related topics, IMS Lecture notes monograph series* (Vol. 28, pp. 120–141). Hayward, CA: Institute of Mathematical Statistics.

Joe, H. (1997). *Multivariate models and multivariate dependence concepts*. Boca Raton, FL: CRC Press.

Khedun, C. P., Mishra, A. K., Singh, V. P., & Giardino, J. R. (2014). A copula-based precipitation forecasting model: Investigating the interdecadal modulation of ENSO's impacts on monthly precipitation. *Water Resources Research*, *50*, 580–600. https://doi.org/10.1002/2013WR013763

Kousky, V. E., & Higgins, R. W. (2007). An alert classification system for monitoring and assessing the ENSO cycle. *Weather and Forecasting*, *22*(2), 353–371. https://doi.org/10.1175/WAF987.1

Kurowicka, D. (2011). *Dependence modeling: Vine copula handbook*. Singapore: World Scientific.

Kurowicka, D., & Cooke, R. M. (2007). Sampling algorithms for generating joint uniform distributions using the vine-copula method. *Computational Statistics & Data Analysis*, *51*(6), 2889–2906. https://doi.org/10.1016/j.csda.2006.11.043

Latif, M., & Keenlyside, N. S. (2009). El Niño/Southern Oscillation response to global warming. *Proceedings of the National Academy of Sciences of the United States of America*, *106*(49), 20578–20583. https://doi.org/10.1073/pnas.0710860105

Leonard, M., Westra, S., Phatak, A., Lambert, M., van den Hurk, B., McInnes, K., et al. (2014). A compound event framework for understanding extreme impacts. *Wiley Interdisciplinary Reviews: Climate Change*, *5*(1), 113–128. https://doi.org/10.1002/wcc.252

Liu, Z., Törnros, T., & Menzel, L. (2016). A probabilistic prediction network for hydrological drought identification and environmental flow assessment. *Water Resources Research*, *52*, 6243–6262. https://doi.org/10.1002/2016WR019106

Liu, Z., Zhou, P., Chen, X., & Guan, Y. (2015). A multivariate conditional model for streamflow prediction and spatial precipitation refinement. *Journal of Geophysical Research: Atmospheres*, *120*, 10116–10129. https://doi.org/10.1002/2015JD023787

Lloyd, C. D. (2005). Assessing the effect of integrating elevation data into the estimation of monthly precipitation in Great Britain. *Journal of Hydrology*, *308*(1), 128–150. https://doi.org/10.1016/j.jhydrol.2004.10.026

Lott, F. C., Christidis, N., & Stott, P. A. (2013). Can the 2011 East African drought be attributed to human-induced climate change?. *Geophysical Research Letters*, *40*, 1177–1181. https://doi.org/10.1002/grl.50235

MacDonald, I. L., & Zucchini, W. (1997). *Hidden Markov and other models for discrete-valued time series*. Boca Raton, FL: CRC Press.

Madadgar, S., AghaKouchak, A., Shukla, S., Wood, A. W., Cheng, L., Hsu, K. L., et al. (2016). A hybrid statistical-dynamical framework for meteorological drought prediction: Application to the southwestern United States. *Water Resources Research*, *52*, 5095–5110. https://doi.org/10.1002/2015WR018547

Madadgar, S., & Moradkhani, H. (2011). Drought analysis under climate change using copula. *Journal of Hydrologic Engineering*, *18*, 746–759. https://doi.org/10.1061/(ASCE)HE.1943-5584.0000532

Madadgar, S., & Moradkhani, H. (2013). A Bayesian framework for probabilistic seasonal drought forecasting. *Journal of Hydrometeorology*, *14*(6), 1685–1705. https://doi.org/10.1175/JHM-D-13-010.1

Meehl, G. A., & Teng, H. (2007). Multi-model changes in El Niño teleconnections over North America in a future warmer climate. *Climate Dynamics*, *29*(7–8), 779–790. https://doi.org/10.1007/s00382-007-0268-3

Min, A., & Czado, C. (2010). Bayesian inference for multivariate copulas using pair-copula constructions. *Journal of Financial Econometrics*, *8*(4), 511–546. https://doi.org/10.1093/jfinec/nbp031

Moftakhari, H. R., Salvadori, G., AghaKouchak, A., Sanders, B. F., & Matthew, R. A. (2017). Compounding effects of sea level rise and fluvial flooding. *Proceedings of the National Academy of Sciences of United Stated of America*, *114*(37), 9785–9790. https://doi.org/10.1073/pnas.1620325114

Mueller, B., & Seneviratne, S. I. (2012). Hot days induced by precipitation deficits at the global scale. *Proceedings of the National Academy of Sciences of United Stated of America*, *109*(31), 12398–12403. https://doi.org/10.1073/pnas.1204330109

National Climate Data Center (NCDC). (2002). *Time bias corrected divisional temperature-precipitation-drought index* (Documentation for dataset TD-9640, 12 p.). Asheville, NC: National Climatic Data Center. Retrieved from http://www1.ncdc.noaa.gov/pub/data/documentlibrary/tddoc/td9640.pdf

Pall, P., Aina, T., Stone, D. A., Stott, P. A., Nozawa, T., Hilberts, A. G., et al. (2011). Anthropogenic greenhouse gas contribution to flood risk in England and Wales in autumn 2000. *Nature*, *470*, 382–385. https://doi.org/10.1038/nature09762

Prosdocimi, I., Kjeldsen, T. R., & Miller, J. D. (2015). Detection and attribution of urbanization effect on flood extremes using nonstationary flood-frequency models. *Water Resources Research*, *51*, 4244–4262. https://doi.org/10.1002/2015WR017065

Ren, X., Li, S., Lv, C., & Zhang, Z. (2014). Sequential dependence modeling using Bayesian theory and D-vine copula and its application on chemical process risk prediction. *Industrial & Engineering Chemistry Research*, *53*(38), 14788–14801. https://doi.org/10.1021/ie501863u

Ropelewski, C. F., & Halpert, M. S. (1986). North American precipitation and temperature patterns associated with the El Niño/Southern Oscillation (ENSO). *Monthly Weather Review*, *114*, 2352–2362. https://doi.org/10.1175/1520-0493(1986)114<2352:NAPATP>2.0.CO;2

Sadegh, M., Ragno, E., & AghaKouchak, A. (2017). Multivariate Copula Analysis Toolbox (MvCAT): Describing dependence and underlying uncertainty using a Bayesian framework. *Water Resources Research*, *53*, 5166–5183. https://doi.org/10.1002/2016WR020242

Salvadori, G., De Michele, C., & Durante, F. (2011). On the return period and design in a multivariate framework. *Hydrology and Earth System Sciences*, *15*, 3293–3305. https://doi.org/10.5194/hess-15-3293-2011

Salvadori, G., De Michele, C., Kottegoda, N. T., & Rosso, R. (2007). *Extremes in nature: An approach using copulas*. Berlin, Germany: Springer Science & Business Media.

Salvadori, G., Durante, F., & Michele, C. (2013). Multivariate return period calculation via survival functions. *Water Resources Research*, *49*, 2308–2311. https://doi.org/10.1002/wrcr.20204

Sarhadi, A., Burn, D. H., Concepción Ausín, M., & Wiper, M. P. (2016). Time-varying nonstationary multivariate risk analysis using a dynamic Bayesian copula. *Water Resources Research*, *52*, 2327–2349. https://doi.org/10.1002/2015WR018525

Schepsmeier, U., Stoeber, J., Brechmann, E. C., Graeler, B., Nagler, T., & Erhardt, T. (2012). *Package VineCopula*. Vienna: R Foundation. Retrieved from https://cran.r-project.org/web/packages/VineCopula/VineCopula.pdf

Schirmacher, D., & Schirmacher, E. (2008). Multivariate dependence modeling using pair-copulas. Paper presented at The 2008 Enterprise Risk Management Symposium, Chicago.

Seneviratne, S. I., Nicholls, N., Easterling, D., Goodess, C. M., Kanae, S., Kossin, J., et al. (2012). Changes in climate extremes and their impacts on the natural physical environment. In C. B. Field et al. (Eds.), *Managing the risks of extreme events and disasters to advance climate change adaption, A special report of working groups I and II of the intergovernmental panel on climate change* (pp. 109–230). Cambridge, UK: Cambridge University Press.

Serinaldi, F., Bonaccorso, B., Cancelliere, A., & Grimaldi, S. (2009). Probabilistic characterization of drought properties through copulas. *Physics and Chemistry of the Earth, Parts A/B/C*, *34*(10), 596–605. https://doi.org/10.1016/j.pce.2008.09.004

Sillmann, J., Kharin, V. V., Zwiers, F. W., Zhang, X., & Bronaugh, D. (2013). Climate extremes indices in the CMIP5 multimodel ensemble: Part 2. Future climate projections. *Journal of Geophysical Research*, *118*, 2473–2493. https://doi.org/10.1002/jgrd.50188

Sklar, A. (1959). Fonctions de répartition á n dimensions et leurs marges. *Publications de l'Institut de Statistique de l'Université de Paris*, *8*, 229–231

Stocker, T. F., Qin, D., Plattner, G. K., Tignor, M., Allen, S. K., Boschung, J., et al. (Eds.) (2013). *IPCC, 2013: Climate change 2013: The physical science basis, Contribution of working group I to the fifth assessment report of the intergovernmental panel on climate change*. Cambridge, UK: Cambridge University Press.

Stott, P. A., Stone, D. A., & Allen, M. R. (2004). Human contribution to the European heatwave of 2003. *Nature*, *432*, 610–614. https://doi.org/10.1038/nature03089

Timmermann, A., Oberhuber, J., Bacher, A., Esch, M., Latif, M., & Roeckner, E. (1999). Increased El Niño frequency in a climate model forced by future greenhouse warming. *Nature*, *398*, 694–697. https://doi.org/10.1038/19505

Trenberth, K. E., Fasullo, J. T., & Shepherd, T. G. (2015). Attribution of climate extreme events. *Nature Climate Change*, *5*(8), 725730. https://doi.org/10.1038/nclimate2657

Vandenberghe, S., Verhoest, N. E. C., Onof, C., & De Baets, B. (2011). A comparative copula-based bivariate frequency analysis of observed and simulated storm events: A case study on Bartlett-Lewis modeled rainfall. *Water Resources Research*, *47*, W07529. https://doi.org/10.1029/2009WR008388

Vernieuwe, H., Vandenberghe, S., De Baets, B., & Verhoest, N. (2015). A continuous rainfall model based on vine copulas. *Hydrology and Earth System Sciences*, *19*(6), 2685–2699. https://doi.org/10.5194/hessd-12-489-2015

Wang, S. Y., Huang, W. R., Hsu, H. H., & Gillies, R. R. (2015). Role of the strengthened El Niño teleconnection in the May 2015 floods over the southern Great Plains. *Geophysical Research Letters*, *42*, 8140–8146. https://doi.org/10.1002/2015GL065211

Webster, P. J. (1981). Mechanisms determining the atmospheric response to sea surface temperature anomalies. *Journal of the Atmospheric Sciences*, *38*(3), 554–571. https://doi.org/10.1175/1520-0469(1981)038<0554:MDTART>2.0.CO;2

Wu, R., Hu, Z. Z., & Kirtman, B. P. (2003). Evolution of ENSO-related rainfall anomalies in East Asia. *Journal of Climate*, *16*(22), 3742–3758. https://doi.org/10.1175/1520-0442(2003)016<3742:EOERAI>2.0.CO;2

Xiong, L., Jiang, C., Xu, C. Y., Yu, K. X., & Guo, S. (2015). A framework of change-point detection for multivariate hydrological series. *Water Resources Research*, *51*, 8198–8217. https://doi.org/10.1002/2015WR017677

Xiong, L., Yu, K. X., & Gottschalk, L. (2014). Estimation of the distribution of annual runoff from climatic variables using copulas. *Water Resources Research*, *50*, 7134–7152. https://doi.org/10.1002/2013WR015159

Yan, J. (2007). Enjoy the joy of copulas: With a package copula. *Journal of Statistical Software*, *21*(4), 1–21. https://doi.org/10.18637/jss.v021.i04